Influence of attached growth on the performance of *Pseudomonas fluorescens* grown on fluoroacetate as the sole organic substrate

Running title: Influence of attached growth on *P. fluorescens*

Barry Heffernan[1], Cormac D. Murphy[2] and Eoin Casey[1]*.

[1]UCD School of Chemical and Bioprocess Engineering, Centre for Synthesis and Chemical Biology, and [2]UCD School of Biomedical and Biomolecular Science, University College Dublin, Belfield, Dublin 4, Ireland.

*Corresponding Author: Eoin Casey.

Address: UCD School of Chemical and Bioprocess Engineering, Engineering and Materials Science Centre, University College Dublin, Belfield, Dublin 4, Ireland.

Email: eoin.casey@ucd.ie

Telephone: +353 1 7161877

Fax: +353 1 7161177

Abstract

Comparisons between the physiological properties of *Pseudomonas fluorescens* biofilm cells grown in a tubular biofilm reactor and planktonic cells grown in a chemostat were performed. Fluoroacetate was the sole carbon source for all experiments. The performance of cells was assessed using cell cycle kinetics and by determining specific fluoroacetate utilization rates. Cell cycle kinetics were studied by flow cytometry in conjunction with the fluorescent stain propidium iodide. Determination of the DNA content of planktonic and biofilm cultures showed little difference between the two modes of growth. Cultures with comparable specific glycolate utilization rates had similar percentage of cells in the B phase of the cell cycle indicating similar growth rates. Specific fluoroacetate utilization rates showed the performance of planktonic cells to be superior to biofilm cells with more fluoroacetate utilized per cell at similar specific fluoroacetate loading rates. A consequence of this decreased biofilm performance was the accumulation of glycolate in the effluent of biofilm cultures. This accumulation of glycolate was not observed in the effluent of planktonic cultures. Spatial stratification of oxygen within the biofilm was identified as a possible explanation for the overflow metabolism of glycolate and the decreased performance of the biofilm cells.

Introduction

There is a general consensus that the adhesion of microbes to a surface influences bacterial metabolism, however the experimental results are often contradictory (34). Some studies have compared the physiological status of biofilm and planktonic cells by determining their growth rates, with some (2, 9) reporting increased biofilm growth rates in comparison to planktonic growth rates, while others (1) have reported the opposite. Other researchers have compared the influence of adhesion on biofilm metabolic activity in comparison with planktonic activity and as with growth rate, conflicting observations have been reported (16, 31, 11). The objective of the present study was to characterise planktonic cells grown in a chemostat and biofilm cells grown in a tubular biofilm reactor (TBR) and compare their performance with respect to the degradation of a model xenobiotic compound fluoroacetate.

Halogenated compounds are extensively used in many applications (refrigeration, lubricants, pharmaceuticals, insecticides and herbicides) and can be considered significant environmental contaminants. The biodegradation of many chlorinated compounds has been widely reported (5, 26, 28). However, considering the increased use of organofluorine compounds in the past 60 years there is limited information on their degradation (17). Currently a large fraction of wastewater streams containing fluorinated compounds are incinerated (12). Improved biological waste treatment processes require a deeper understanding of microbial degradation of fluorinated compounds.

Some previous studies have focused on the biodegradation of fluorinated aromatic compounds using biofilm reactors (3, 10); however, there have been no studies on the degradation of fluorinated aliphatic compounds in biofilm reactors. Thus sodium fluoroacetate was chosen as the model xenobiotic to study the efficiency of aliphatic organofluorine degradation in biofilms. It was the first naturally occurring fluorinated

compound to be isolated, from the South African shrub *Dichapetalum cymosum* (23). Fluoroacetate is highly toxic to mammals and has found extensive use as a vertebrate pesticide, particularly in Australia and New Zealand. A number of studies have focused on the isolation and identification of microbial soil isolates with the ability to degrade fluoroacetate (14, 33, 35), and other studies have focused on the mechanism of defluorination (13, 15, 21). However, there has been no research on the degradation of fluoroacetate by biofilm cultures.

Biofilm systems appear ideal for the degradation of xenobiotics considering the many reported advantages they have over planktonic cultures. Most microorganisms that have the ability to degrade xenobiotic compounds have comparatively slow growth rates and biofilm reactors allow the enrichment of these microorganisms independent of hydraulic retention time (36). It has been shown in numerous studies that biofilms are less susceptible to changes in environmental conditions such as temperature, pH, metabolic products and toxic substances than suspended bacteria (8, 25, 27, 36). The high cell concentrations that can be achieved in biofilm systems in combination with high volumetric flow rates could potentially result in high volumetric productivities without the risk of cell washout.

The species *Pseudomonas fluorescens* has been extensively studied and commonly exists as biofilm in natural environments and is ubiquitous in industrial environments (6, 29, 30). The specific strain used here *P. fluorescens* DSM 8314, was previously isolated from a soil sample in Western Australia, and in a study with 23 other microbial soil isolates was shown to be the most efficient degrader of fluoroacetate, when fluoroacetate was the sole carbon source (6, 29, 30, 37). The effect of the environmental factors, pH and temperature, on the biodefluorination of fluoroacetate by *P. fluorescens* was also determined (38); however, at present there are no reported planktonic growth kinetics established for this strain nor has it previously been grown as a biofilm. In this context a tubular biofilm reactor (TBR) was employed to investigate the degradation of fluoroacetate by a *P. fluorescens* biofilm, in

conjunction with chemostat studies, which were conducted to determine the efficiency of planktonic degradation of the substrate. Specific utilization rates, flow cytometry and fluorescent microscopy were employed to compare the performance and physiological status of biofilm and planktonic cells grown with fluoroacetate as the sole organic substrate.

Materials and Methods

Medium and culture conditions.

Pseudomonas fluorescens (DSM 8341) was obtained from the German Collection of Microorganisms and Cell Cultures (DSMZ, Germany). Brunners minimal medium (DSMZ, medium 457) supplemented with sodium fluoroacetate (Sigma, UK) as the sole organic substrate was the growth medium for all experiments with the exception of the 50 mM biofilm experiments. In these experiments the concentration of KH_2PO_4 was increased from 1.52 to 15.2 g/l in order to provide greater buffering capacity.

Biofilm reactor

The biofilm was grown in the lumen of a silicone tube (Alteil^{TM}, UK) referred to as a tubular biofilm reactor (TBR), which is schematically presented in Fig 1. The nominal inner dimension of the silicone tubing was 3 mm and the wall thickness was 1 mm. The system consisted of a medium reservoir, peristaltic pump, a glass flow break, four 40 cm sections of silicone tubing separated by 5 sample ports, a glass flow break and a spent medium reservoir. This reactor configuration allowed the determination of local metabolite concentrations and biofilm characteristics and thus each section can be considered an independent reactor. Four separate TBR experiments were performed, with concentrations of 10, 20 and 50 mM fluoroacetate in the medium feed; the 20 mM experiment was repeated. Thus 16 different specific fluoroacetate loading rates were examined (four reactors with four sections each). Cells were grown for 24 h at 30 ºC in batch culture prior to reactor inoculation to ensure the cells were in the exponential phase of growth. The 24 h culture was adjusted to a turbidity of approximately 0.1 at 660 nm in phosphate-buffered saline (PBS), mixed with 10 ml of medium, and inoculated into the reactor. Following inoculation the system was operated in static mode for approximately 48 h at 30 ºC after which time the flow of medium was initiated

126 at a flow rate of 6 ml/h (velocity 0.023 cm/s) and maintained throughout the experiments. The
127 dilution rate was approximately 2.5 times greater than the maximum planktonic growth rate;
128 this was chosen to ensure the washout of planktonic cells and encourage biofilm formation.
129 The reactor was sampled daily from sample port 5 and from all five ports 24 h prior to biofilm
130 harvesting. The following parameters were analysed: optical density, fluoroacetate, free
131 fluoride ion, glycolate, DNA content of cells and CFUs. The biofilm was allowed to develop
132 for approximately 300 h, at which time the bioreactor was disassembled and the biofilm was
133 harvested for analysis.

134 **Biofilm harvesting**

135 Prior to biofilm harvesting the TBR was drained of bulk liquid to prevent any interference of
136 detached cells. Biofilm cells were harvested from the inside of the tubing which was
137 sectioned into 5 cm divisions with thickness, dry weight, DNA content of cells, and CFUs
138 being measured. Biofilm was removed from the lumen of the tubing by pinching the outer
139 surface of the tubing, the lumen was washed with (PBS) and the disrupted biofilm was
140 harvested.

141 **Chemostat trials**

142 Chemostat studies were performed in duplicate in a 3 l bioreactor (Applikon, The
143 Netherlands) with a working volume of 1.5 l and the performance of planktonic cells was
144 assessed at four fluoroacetate loading rates representing growth rates between 45 and 80 % of
145 the maximum growth rate. The reactor was equipped with controls for agitation, pH,
146 temperature and dissolved oxygen. For pH adjustment 1 M NaOH was used. The inlet gas
147 flow rate was maintained at a constant rate of 1.5 l/min by use of a mass flow controller.
148 Dissolved oxygen was controlled by agitation and maintained at or above 40 % air saturation
149 throughout the experiments. Temperature was maintained at 30 ºC throughout the
150 experiments. The reactor was inoculated with 15 ml of 24 h old culture adjusted to an optical

density of 0.1 at 660 nm. The reactor was sampled periodically and the following parameters were analysed: optical density, fluoroacetate, free fluoride ion, glycolate, DNA content of cells, dry weight and CFUs. The reactor was operated under batch conditions during the exponential phase of growth, at the onset of the stationary phase of growth the reactor was switched to continuous operation. The feed flow rate was measured by recording the mass of liquid effluent over a specified period of time using a balance (Mettler Toledo, USA). The initial fluoroacetate concentration during the batch phases of growth was 20 mM.

Batch growth trials

Planktonic growth rates were determined for initial fluoroacetate concentrations of 10, 20 and 50 mM in 250 ml conical flasks incubated at 30 ºC with shaking at 150 rpm. The flasks were operated with a working volume of 50 ml and inoculated with a 0.5 ml of a 24 h old culture adjusted to an optical density of 0.1 at 660 nm with PBS. The flasks were sampled periodically and analysed for optical density and free fluoride ion.

Anaerobic batch culture experiments

Anaerobic batch culture experiments were performed in triplicate with 20 mM of fluoroacetate or 20 mM of glycolate respectively as the sole carbon source in 100 ml Schott Duran bottles with a working volume of 30 ml. An anaerobic environment was maintained by continuous subsurface sparging of nitrogen gas at a flow rate of 0.5 ml/min. This flow rate was found to be sufficient to ensure an anaerobic environment while also avoiding liquid losses due to evaporation over the 8 h duration of the experiment. The Duran bottles were inoculated by harvesting 30 ml of a 24 h old culture grown on fluoroacetate; the harvested cells were then resuspended in 1 ml of fresh media prior to inoculation. The bottles were incubated at 30 ºC with shaking at 150 rpm for 8 h at which time they were sampled and analysed for optical density, dissolved oxygen and metabolite concentrations. After the 8 h incubation period the dissolved oxygen concentration was measured in both the anaerobic and

aerobic experiments. There was no dissolved oxygen detected in any of the anaerobic experiments while the dissolved oxygen concentrations in the aerobic control bottles were found to be above 40 % air saturation after the 8 h incubation period.

Epifluorescence microscopy

A 5 cm section of tubing containing biofilm was washed with PBS (1 ml) and stained with 5-cyano-2,3-ditoyl tetrazolium chloride (CTC; 400 µg/ml), for 2 h at 30 ºC. The tubing was drained, washed with PBS (1 ml) and stained with 4'-6-diamidino-2-phenylindole (DAPI; 100 µg/ml), for 30 min at ambient temperature. The tubing was washed with PBS and embedded with 5 ml of O.C.T. histological cryoembedding medium (Tissue-TEK O.C.T. compound), which was gently injected into the tubing. The tubing was then placed in an embedding chamber for 10 min to solidify the O.C.T. and samples were stored at – 80 ºC until sectioning. The embedded biofilm was sectioned (10 µm cross sections), after removing the biofilm from the silicone tubing, using a Microm HM 550 cryostat (Microm, Walldorf, Germany). The sections were placed on glass slides and examined with an Olympus BX51 epifluorescence microscope using a 4-x objective. Photographs were obtained with an Olympus DP70 digital camera. The exposure time when acquiring CTC images was 500 ms, and 50 ms when acquiring DAPI images.

Thickness measurements and image analysis

Biofilm thickness was analysed by Able Image Analyser software (Mu Labs, Slovenia). Thickness was measured as the distance from the membrane to the biofilm liquid interface. From each section of the reactor six phase contrast images were analysed for thickness with 25 measurements taken from each image. These measurements were then averaged to give a final thickness. Depth profiles of respiratory activity (CTC) and biomass (DAPI) were measured perpendicular to the membrane in overlapped CTC and DAPI images acquired at the same point. The interface between the biofilm and the membrane was set at zero. Fifteen

individual profiles were performed in six different images from each section. Three representative profiles were then averaged to produce a final radial profile of respiratory activity and biomass for each section

Dry weight

Biofilm dry weight was determined by drying a 5 cm section of tubing at 60 ºC for 48 h, at which point a constant weight was achieved. The tubing was immersed in warm water to hydrate the biofilm, and the biofilm was removed by pinching the silicone tubing, which was then washed vigorously with water to remove any residual biofilm. The silicone tubing was dried for a further 48 h and reweighed. The weight of the biofilm was calculated by subtracting the dry weight of the empty tubing from the weight of the tubing plus biofilm.

Specific utilization rate

The specific utilization rate (q) is defined as the concentration of substrate degraded per unit time per CFU. The utilization of a carbon/energy substrate is separated into two fluxes (Fig 2) corresponding to consumption of the substrate for incorporation into biomass (q_{an}) and utilization of substrate for energy which can be further subdivided into the energy required for growth (q_{en}) and energy required for maintenance (q_m). In some cases it is possible that there is a rate-limiting step in the overall catabolic pathways, which leads to the accumulation of an intermediate metabolite and is described here as overflow metabolism (Om). Fluoroacetate was the sole organic substrate available to the cells and is initially degraded by the enzyme fluoroacetate dehalogenase (Fig 3), yielding free fluoride ion and glycolate; glycolate is then utilized as the carbon/energy source. Figure 3 shows that carbon is conserved in the fluoroacetate dehalogenase reaction thus there are two specific utilization rates q_f, which is the specific utilization rate of fluoroacetate, which is a single enzymatic reaction, and results in the production of glycolate, and q_g, the specific utilization rate of glycolate consumed for the production of cell material (q_{an}) and ATP generation (q_{en} and q_m). Unconsumed

glycolate (Om) is transported across the cell membrane into the bulk liquid. In order to compare q_f and q_g directly specific utilization rates were calculated in mM carbon.

Flow cytometry

Cells were harvested from biofilm and planktonic cells as described, diluted to a concentration of approximately 5×10^6 cells per ml and washed three times in PBS. This was performed by re-suspending the biofilm in PBS, centrifuging for 5 min at 14,000 rpm and discarding the supernatant. The washed cells were suspended in 0.1 ml of PBS and 1 ml of ice-cold 70% ethanol. The cells were kept at 4 ºC for 24 h to fix the cells prior to transfer to – 20 ºC for storage. Prior to analysis the cells were separated from the ethanol by centrifugation and re-suspended in 1 ml of PBS containing propidium iodide (80 μM). Cells were then analysed for DNA content using a Dako Cyan ADP flow cytometer (Dako, Glostrup, Denmark) and histograms showing fluorescence intensity against cell number were generated (Fig 4). The different phases of cell cycle (B, C and D) were then determined from these histograms using Multicycle software (Phoenix Flow Systems, USA).

Fluoroacetate, free fluoride ion and glycolate analysis

Free fluoride ion was measured using an ion selective fluoride combination electrode (Thermo Orion model 290). Fluoroacetate concentration was determined by fluorine-19 nuclear magnetic resonance (^{19}F NMR) spectroscopy. Samples were prepared by mixing 0.6 ml of culture fluid with 0.2 ml D_2O (added to provide a lock signal) and analysis was performed using a Varian 400 MHz spectrometer. The known free fluoride concentration in each effluent sample was used as an internal standard. The ratio of free fluoride ion signal (-120 ppm) to fluoroacetate signal (- 215 ppm) was used to calculate fluoroacetate concentration. Glycolate was measured by the method described by (20).

Results

Biofilm formation, growth and structural characteristics

The TBR system was employed as a method to characterise *P. fluorescens* biofilms grown at varying carbon loading rates. Carbon loading rate is defined here as the total carbon available in a section of tubing, it includes both the carbon in the form of fluoroacetate and the carbon in the form of glycolate. It has been shown that fluid velocity is a critical parameter in determining biofilm adhesive strength for *P. fluorescens* biofilms (4), accordingly in order to maintain a constant velocity in all experiments carbon loading rates were varied by altering the fluoroacetate inlet medium concentration and not the dilution rate. Experiments were performed with initial fluoroacetate concentrations of 10, 20 and 50 mM in the medium feed. Visual observation of initial biofilm formation occurred between 116 and 160 h after reactor inoculation. Biofilm appearance, as indicated by colony formation on the lumen of the silicone tube, depended on the carbon loading rate; in experiments employing 10 and 20 mM fluoroacetate, where carbon loading rates were between 0 and 0.190 mM/h, biofilm growth was apparent in a shorter period of time than in experiments with 50 mM fluoroacetate, where carbon loading rates were between 0.300 and 0.510 mM/h. Steady state, as indicated by fluoroacetate, glycolate and free fluoride ion concentrations in the effluent, was achieved earlier in the experiments with lower carbon loading rates. In the reactors with initial carbon loading rates of less than 0.190 mM/h, complete carbon utilization had occurred by the time steady state had been reached. However, in the reactor with carbon loading rates of above 0.300 mM/h approximately 3 mM of fluoroacetate and 18 mM of glycolate were still detectable at steady state.

Visual observations of the biofilm formation provides some qualitative information as to when initial biofilm formation occurs and measured metabolite concentrations throughout

276 the time course of the experiments indicate when steady state conditions have been reached,
277 but these data do not provide any quantitative measurement of biofilm structure or
278 performance. Thus, biofilm characteristics of thickness, dry weight, cell number and density
279 were calculated at different sections of the reactor (Fig 1), for different carbon loading rates
280 after biofilm harvesting (Table 1). Cross sectional biofilm thickness was calculated from
281 phase contrast images. These thickness measurements show little variation in the average
282 biofilm thickness for all sections where the carbon-loading rates was above 0.017 mM/h
283 where the average was 116.8 μm with a standard deviation around the mean of ± 22.9 μm. An
284 exception to this trend was the section with a carbon loading rate of 0.107 mM/h where the
285 average thickness was 130 μm thicker than that recorded in any other section. The same
286 trends observed for average thickness were observed for dry weight, CFU and density
287 measurements with a few exceptions most notably for the section with a carbon loading rate
288 of 0.107 mM/h. Images taken from the section with this carbon loading rate suggest that the
289 biofilm may have been in the process of sloughing and this could explain the greater thickness
290 and lower density values recorded in this section. The 20 mM reactor experiment was
291 performed in duplicate, and Anova single factor statistical analysis showed that there was no
292 significant difference between biofilm thickness, dry weight, cell number and density values
293 recorded in these two reactors ($F= 0.15$, $F_{crit}=4.7$ and $p=0.69$). Biofilm was present in three
294 individual sections of the reactors where the carbon loading rate was 0 mM/h, on account of
295 carbon source depletion and in these sections the presence of biofilm was probably a result of
296 carbon being present during the early stages of the reactor operation.

297 **Comparisons between planktonic and biofilm performance**

298 Comparisons between biofilm and planktonic cells are difficult to make due to the intrinsic
299 difference between the two modes of growth, such as compositional differences in biomass.
300 Typically, performance is determined by specific utilization rates (q), where q is defined as

301 the concentration of substrate degraded per unit time divided by the dry weight of biomass.
302 However, dry weight measurements do not take into account EPS, which will account for a
303 much higher fraction of biofilm biomass than it will for planktonic biomass. It has been
304 demonstrated that the composition of *P. fluorescens* B52 extracellular polymeric substances
305 (EPS) is different for biofilm and planktonic cells (18). Thus, in this study q was calculated
306 using CFUs rather than dry weight. CFU measurements are advantageous in this situation as
307 they are a measure of viable cells for both biofilm and planktonic systems. The reactor
308 working volume for the chemostat was 1.5 l while the reactor volume in each section of the
309 TBR was only 0.0028 l. To account for this difference in reactor volumes, specific
310 fluoroacetate loading rates (mM/CFU h), rather than fluoroacetate loading rates (mM/h), were
311 used in conjunction with specific fluoroacetate and glycolate utilization rates to compare the
312 performance of biofilm and planktonic cells (Fig 5). For the range of loading rates
313 investigated the data clearly reflect higher utilization rates for planktonic cells than for biofilm
314 cells. Linear regression analysis of fluoroacetate utilization rates at specific fluoroacetate
315 loading rates between 0 and 14×10^{-12} mM/CFU h show a linear relationship for both biofilm
316 (R^2=0.91) and planktonic cells (R^2=0.90). Biofilm fluoroacetate loading rates above 14×10^{-12}
317 mM/CFU h were not included in the regression analysis as the performance of planktonic
318 cells was not assessed above this range. The performance of planktonic cells was superior to
319 biofilm cells with a higher dependency of specific fluoroacetate utilization recorded for
320 planktonic cells (slope=0.87) than for biofilm cells (slope=0.57). Specific glycolate utilization
321 rates for planktonic cells were the same as specific fluoroacetate utilization rates, thus the
322 fluoroacetate degradation/glycolate production rate was equal to the rate of glycolate
323 utilization for planktonic cells at all specific fluoroacetate loading rates examined. However,
324 there were significant differences between specific glycolate and specific fluoroacetate
325 utilization rates for biofilm cells at all specific fluoroacetate loading rates above 2×10^{-12}

326 mM/CFU h (t-stat=1.43, p=0.091) (based on a one-tailed t-test, assuming unequal variances).
327 A result of this difference between specific fluoroacetate and glycolate utilization rates for
328 biofilm cells was the accumulation of glycolate (overflow metabolism). Thus, the data
329 indicate a rate-limiting step in the utilization of glycolate by biofilm cells that was not
330 observed for planktonic cells.

331 **Oxygen limitation**

332 Depth profiles of respiratory activity as indicated by CTC and biomass concentration as
333 indicated by DAPI show spatial stratification of respiratory activity within the biofilm (Fig 6).
334 The region of highest respiratory activity is located adjacent to the biofilm membrane
335 interface where oxygen concentration is highest. Respiratory activity decreases towards the
336 bulk liquid interface while biomass concentration does not, suggesting decreased oxygen
337 availability in this location. While it was not possible to measure the oxygen profiles within
338 the biofilm in this study, the penetration depth of oxygen into a biofilm is governed by a
339 reaction-diffusion interaction. The relative rate of oxygen diffusion and oxygen consumption
340 by the biofilm determines the depth of oxygen penetration, which can be determined
341 theoretically from the following equation (32): $a = (2D_e S_o / k_o)^{1/2}$, where a is the
342 penetration depth of the reacting solute, D_e is the effective diffusion coefficient of the solute
343 in the biofilm, S_o is the solute concentration at the biofilm interface and k_o is the volumetric
344 reaction rate of the solute inside the biofilm. Estimates of each of these parameters were made
345 to allow the calculation of oxygen penetration depth. The effective diffusion coefficient of
346 oxygen in the biofilm at 30 °C was taken as 57% of the diffusion coefficient of pure water at
347 this temperature (32), or $1.28 \times 10^{-5}\,\mathrm{cm^2 s^{-1}}$. The concentration of dissolved oxygen at the
348 biofilm membrane interface was taken as 8.0 mg litre^{-1}, and the volumetric consumption rate
349 of oxygen was determined experimentally to be 1.64 mg litre^{-1} s^{-1}. From these estimates the
350 calculated depth of oxygen penetration into the biofilm from the membrane was 111 μm. The

351 average biofilm thickness in the sections of the reactors where overflow metabolism of
352 glycolate occurred was 118 μm ± 21 μm. These oxygen depth calculations combined with
353 biofilm thickness measurements and the spatial stratification of respiratory activity within the
354 biofilm suggest that oxygen does not completely penetrate into the biofilm. A study by (7)
355 demonstrated that the fluoroacetate dehalogenase enzyme isolated from *P. fluorescens* does
356 not require the presence of oxygen to degrade fluoroacetate. Thus, a possible explanation for
357 the overflow metabolism of glycolate is oxygen limitation. Anaerobic batch culture
358 experiments were performed to test the hypothesis that oxygen limitation was the reason for
359 the overflow metabolism of glycolate in the TBR. There was no growth, as indicated by
360 optical density measurements, in either the fluoroacetate or glycolate anaerobic bottles after 8
361 h of incubation, demonstrating that oxygen is require for biomass production. However, when
362 the cells were incubated with fluoroacetate under anaerobic conditions 1.2 ± 0.01 mM of
363 glycolate and 1.4 ± 0.05 mM of free fluoride ion were detected in the effluent. Thus,
364 fluoroacetate was degraded in the absence of oxygen but glycolate was not and the data there
365 by supports the possibility that oxygen is the rate limiting step in overall glycolate catabolism.
366 Interestingly, when *P. fluorescens* was grown aerobically there was greater biomass
367 production when the cells were grown on glycolate as the sole carbon source (O.D 0.811 ±
368 0.11) than when the sole carbon source was the fluoroacetate (O.D 0.411 ± 0.16), the OD at
369 time 0 was 0.150 for all experiments. The cells grown on glycolate utilized more carbon (16.2
370 ± 0.3 mM) than cells grown on fluoroacetate (8.5 ±0.45 mM) in the same time period which is
371 surprising considering the cells were adapted to growth on fluoroacetate and not glycolate. As
372 with the shake flask and chemostat experiments, no glycolate was detected in the effluent of
373 the control fluoroacetate aerobic experiment indicating that the fluoroacetate degradation rate
374 was equal to the glycolate utilization rate when oxygen is not limiting.

Comparisons between the DNA content of planktonic and biofilm cells

Bacteria with doubling times between 0.3 and 1 h can have multiple copies of DNA making cell cycle analysis difficult due to overlapping replication cycles. Batch culture planktonic growth trials were performed to determine the doubling times of *P. fluorescens* grown on 10, 20 and 50 mM fluoroacetate, and were found to be 8.3, 6.6 and 7.1 hours, respectively. The B-phase of the bacterial cell cycle can be described as the time between cell division and the initiation of a new round of replication; the C-phase is the time between initiation and termination of chromosome replication; and the D-phase is the time between chromosome termination and cell division. The C and D-phases of growth can be considered constants. However, at growth rates of less than 1 doubling per hour the B-phase of bacterial growth is not constant but increases with decreasing growth rate, thus an increase in the percentage of cells in a population in the B-phase can be expected in slowly growing cells (19). The distributions of biofilm and planktonic cells in the various phases of cell cycle (B, C and D) are compared with specific glycolate utilization rates (Fig 7). Cell cycle distributions were compared using specific glycolate utilization rates and not specific fluoroacetate utilization rates, as the former is a measurement of the utilization of substrate for carbon and energy, while the latter is a measurement of a single enzyme activity. Biofilm and planktonic cells that had zero specific glycolate utilization rates (zero carbon loading rates) as expected have a very high percentage of cells in the B phase (approximately 90 %), while there were very few cells in the D phase of cell cycle. On the basis on a one-tailed t-test, assuming unequal variances, the data shows that, for biofilm cells, increased specific glycolate utilization rates from between 0.06 and 2×10^{-12} mM/CFU h to between 4.5 and 8×10^{-12} mM/CFU h significantly increases the percentage of cells in the B (t-stat=3.98, p=0.00266). No carbon in the form of either fluoroacetate or glycolate was detected in the effluent of these sections and thus, it is probable that these cells had decreased growth rates, of less than 0.1 h^{-1}, as a result

of carbon limitation. The data suggest that there is no significant difference between the percentage of cells in the B phase of growth for planktonic and biofilm cells, investigated at similar specific glycolate utilization rates between 4 and 8 x 10^{-12} mM/CFU h (t-stat=0.25, p=0.403), suggesting that the two populations of cells have similar growth rates between 0.1 and 0.12 h^{-1} (based on a one-tailed t-test, assuming unequal variances). There was a statistically significant decrease in the percentage of cells in the B phase of growth when planktonic specific glycolate utilization rates increased from between 4 and 8 x 10^{-12} mM/CFU h to between 8 and 12 x 10^{-12} mM/CFU h (t-stat=1.57, p=0.09) (based on a one-tailed t-test, assuming unequal variances). This decrease in the percentage of cells in the B phase was as expected, as the cells with specific glycolate utilization rates between 8 and 12 x 10^{-12} mM/CFU h are utilizing more carbon, have higher growth rates between 0.14 and 0.18 h^{-1} and consequently have fewer cells in the B phase of growth as opposed to the cells with specific glycolate utilization rates between 4 and 8 x 10^{-12} mM/CFU h where the growth rates were between 0.1 and 0.12 h^{-1}.

Discussion

The increasing number of applications that rely on organofluorine compounds has resulted in them becoming universal environmental contaminants (24). However the degradation of fluorinated xenobiotics is poorly understood in comparison to other halogenated compounds, where research has tended to concentrate on chlorinated and brominated pollutants. Biodegradation pathways can result in the accumulation of intermediates that are potentially inhibitory or toxic (22), and because of the importance of diffusion in biofilms the accumulation of such intermediates could potentially affect performance. The biodegradation of the model xenobiotic, fluoroacetate, by *P. fluorescens* was investigated and comparisons between the performance of planktonic and biofilm cells were made.

Here two methods have been used to determine the physiological status and activity of planktonic and biofilm cells. First, the metabolic activity of biofilm and planktonic cells were assessed in terms of specific utilization rates. It was found that the performance of planktonic cells was superior to biofilm cells with planktonic cells mineralizing more fluoroacetate per CFU per hour than the biofilm cells. When the cells were grown under planktonic conditions there was no difference between specific fluoroacetate and specific glycolate utilization rates at any of the specific fluoroacetate loading rates examined (Fig 5). This was not the case for the biofilm cells, and specific glycolate utilization rates were decreased in comparison to their corresponding specific fluoroacetate utilization rates at a number of specific fluoroacetate loading rates. Thus, the major differences between biofilm and planktonic cells were the decreased performance of the biofilm cells in terms of fluoroacetate and glycolate utilization and the overflow metabolism of glycolate.

It has been shown previously by (7) that the fluoroacetate dehalogenase enzyme isolated from *P. fluorescens* does not require the presence of oxygen to degrade fluoroacetate and in this study it has been demonstrated that the utilization of glycolate via aerobic

450 respiration requires oxygen as a terminal electron acceptor. Thus, oxygen limitation within the
451 biofilm offers an explanation for the overflow metabolism of glycolate. Spatial stratification
452 of respiratory activity, as indicated by CTC, supports the possibility of oxygen limitation
453 within the biofilm. Respiratory activity is highest at the biofilm/membrane-interface and
454 decreases towards the biofilm/bulk liquid interface (Fig 6). This spatial stratification of
455 nutrients within the biofilm is a major difference between biofilm and planktonic cells. For
456 planktonic cells grown in the chemostat system the dissolved oxygen concentration was
457 controlled at or above 2.8 mg/l, providing sufficient oxygen for all cells. Oxygen was
458 supplied to the biofilm by diffusion through the silicone membrane, which also acts as a
459 support for the biofilm. As the biofilm grows it increasingly acts to resist the mass transfer of
460 nutrients to the inner regions of the biofilm. Calculations of oxygen penetration depth suggest
461 that the biofilm was sufficiently thick to prevent the penetration of oxygen to the region of the
462 biofilm located adjacent to the bulk liquid interface and support the possibility of oxygen
463 limitation.

464 At similar specific fluoroacetate loading rates the specific utilization rate of
465 fluoroacetate was decreased for biofilm cells in comparison to planktonic cells. A possible
466 explanation for this result is the decreased energy available to biofilm cells due to decreased
467 glycolate utilization, thus there is less energy produced for, among other requirements, the
468 production of fluoroacetate dehalogenase, and for the production of any permease necessary
469 for the transport of fluoroacetate into the cell. Therefore, a reduced glycolate utilization rate
470 due to oxygen limitation could ultimately affect fluoroacetate utilization. Decreased energy
471 availability for the transport of fluoroacetate into the cell during anaerobic growth may also
472 offer an explanation as to why only 1.4 mM of fluoroacetate was degraded under these
473 conditions when 8.5 mM was degraded in the same time period under aerobic conditions.

Cell cycle distributions show that there was no statistical difference in the percentage of cells in the B phase of growth at specific glycolate utilization rates between 4 and 8×10^{-12} mM/CFU h for both biofilm and planktonic cells suggesting similar growth rates (Fig 7). If biofilm growth rates of biofilm cells were decreased in comparison to planktonic cells at similar specific glycolate utilization rates, then an increase in the number of cells occupying the B phase of growth would be expected. This was not the case and the cells can be considered to be in a similar physiological state. While some biofilm populations had increased percentages of cells in the B phase of the cell cycle, these increases were probably due to carbon limitation as a result of the low carbon loading rates, between 0.06 and 2×10^{-12} mM/CFU h, in these sections and not as a result of any intrinsic differences between the two modes of growth. The planktonic system was not operated at these low carbon loading rates, and consequently it was not possible to make comparisons between the two modes of growth at these low carbon loading rates.

In conclusion the TBR was found to be a versatile system for determining the performance of biofilm cells. The TBR allows the determination of local metabolite concentrations and other parameters such as dry weight, CFUs, and biofilm thickness which can then be use to assess biofilm performance. While other commonly used biofilm reactor systems such as the rotating disk reactor, the capillary biofilm reactor, and the drip flow biofilm reactor allow the determination of some of these parameters, none allow the determination of so many parameters simultaneously. The identification of the overflow metabolism in biofilm systems could have important implications in the treatment of wastewater streams containing fluorinated compounds. In this case the overflow product was glycolate. Glycolate subsequently acts as the carbon source and did not have any detrimental effect on performance. However, the degradation of other fluorinated compounds, such as fluoroaromatics, might result in the accumulation of toxic fluorometabolites, e.g.

fluorocatechol, which could detrimentally affect the performance of biofilm cells. Planktonic cells were found to be superior to biofilm cells at degrading the xenobiotic with higher fluoroacetate and glycolate utilization rates per CFU recorded at similar specific fluoroacetate loading rates. This difference in performance can be explained by oxygen limitation in the biofilm; however the high free fluoride concentrations recorded in the TBR may also have a negative impact on performance. These results show that while planktonic cells were more efficient at utilizing both fluoroacetate and the intermediate metabolite glycolate, the advantages of biofilm systems for the degradation of xenobiotics, such as the enrichment of slow growing species, may outweigh the superior performance of planktonic cells observed here.

Acknowledgements

We thank Alfonso Blanco for his flow cytometry expertise and Yannick Ortin for ^{19}F NMR analysis. We would like to thank Science Foundation Ireland (SFI) grant 04/BRG/E0072 for their financial support.

References

1. **Barton, A. J., R. D. Sagers, and W. G. Pitt.** 1996. Measurement of bacterial growth rates on polymers. J of Biomed Mater Res **32:**271-278.
2. **Bester, E., G. Wolfaardt, L. Joubert, K. Garny, and S. Saftic.** 2005. Planktonic-cell yield of a *Pseudomonad* biofilm. Appl Environ Microbiol. **71:**7792-7798
3. **Carvalho, M. F., R. Ferreira Jorge, C. C. Pacheco, P. De Marco, and P. M. L. Castro.** 2005. Isolation and properties of a pure bacterial strain capable of fluorobenzene degradation as sole carbon and energy source. Environ Microbiol **7:** 294-298.
4. **Chen, M. J., Z. Zhang, and T. R. Bott.** 2005. Effects of operating conditions on the adhesive strength of *Pseudomonas fluorescens* biofilms in tubes. Colloids Surf B-Biointerfaces **43:**61-71.
5. **Chung, J., B. Rittmann, W. Wright, and R. Bowman.** 2007. Simultaneous bio-reduction of nitrate, perchlorate, selenate, chromate, arsenate, and dibromochloropropane using a hydrogen-based membrane biofilm reactor. Biodegradation **18:**199-209.

6. **Costerton, J. W., Z. Lewandowski, D. E. Caldwell, D. R. Korber, and H. M. Lappin-Scott.** 1995. 1995. Microbial biofilms. Annual Rev Microbiol. **49:**711-745.
7. **Donnelly C, and C. D. Murphy.** 2009. Purification and properties of fluoroacetate dehalogenase from Pseudomonas fluorescens DSM 8341. Biotechnol Lett (in press 10.1007/s10529-008-9849-4).
8. **Duddles, G. A., S. E. Richardson, and E. F. Brath.** 1974. Plastic medium trickling filters for biological nitrogen control. Journal of the Water Pollution Control Federation **46** 937–946.
9. **Ellwood, D. C., C. W. Keevil, P. D. Marsh, C. M. Brown, J. N. Wardell, and N. L. Roux.** 1982. Surface-associated growth [and discussion]. Philos Trans R Soc Lond B Biol Sci. **297:** 517-532.
10. **Emanuelsson, M. A. E., I. S. Henriques, R. M. Ferreira Jorge, and P. M. L. Castro.** 2006. Biodegradation of 2-fluorobenzoate in upflow fixed bed bioreactors operated with different growth support materials. J Chem Technol Biotechnol **81:**1577-1585.
11. **Fletcher, M.** 1986. Measurement of glucose utilization by *Pseudomonas fluorescens* that are free-living and that are attached to surfaces. Appl Environ Microbiol. **52:** 672-676.
12. **Freitas dos Santos, L. M., A. Spicq, A. P. New, G. Lo Biundo, J. C. Wolff, and A. Edwards.** 2001. Aerobic biotransformation of 4-fluorocinnamic acid to 4-fluorobenzoic acid. Biodegradation **12:**23-29.
13. **Goldman, P.** 1965. The enzymatic cleavage of the carbon-fluorine bond in fluoroacetate. J Biol Chem. **240:**3434-3438.
14. **Hamilton, D. J., and C. T. Eason.** 1994. 1994. Monitoring for 1080 residues in waterways after arabbit-poisoning operation in Central Otago. NZ J of Agricul Res. **37:**195-198.
15. **Ichiyama, S., T. Kurihara, Y. Kogure, S. Tsunasawa, H. Kawasaki, and N. Esaki.** 2004. Reactivity of asparagine residue at the active site of the D105N mutant of fluoroacetate dehalogenase from *Moraxella* sp. B. Biochim Biophys Acta **1698:**27-36.
16. **Jeffrey, W. H., and J. H. Paul.** 1986. Activity of an attached and free-living *Vibrio* sp. as measured by thymidine incorporation, p-iodonitrotetrazolium reduction, and ATP/DNA ratios. Appl Environ Microbiol. **51:** 150-156.
17. **Key, B. D., R. D. Howell, and C. S. Criddle.** 1997. Fluorinated organics in the biosphere. Environ Sci Technol. **31:**2445-2454.
18. **Kives, J., B. Orgaz, and C. SanJose.** 2006. Polysaccharide differences between planktonic and biofilm-associated EPS from *Pseudomonas fluorescens* B52. Colloids Surf B-Biointerfaces. **52:**123-127.
19. **Lewin, B.** 2000. Genes IV. Oxford University Press Inc., New York: p.370-371.
20. **Lewis, K., and W. S.** 1957. Determination of glycolic, glyoxylic, and oxalic acids Methods in enzymol. **3:**269-276.
21. **Liu, J.-Q., T. Kurihara, S. Ichiyama, M. Miyagi, S. Tsunasawa, H. Kawasaki, K. Soda, and N. Esaki.** 1998. Reaction mechanism of fluoroacetate dehalogenase from *Moraxella* sp. B. J Biol Chem. **273:**30897-30902.
22. **Luli, G. W., and W. R. Strohl.** 1990. Comparison of growth, acetate production, and acetate inhibition of *Escherichia coli* strains in batch and fed-batch fermentations. Appl Environ Microbiol. **56:**1004-1011.
23. **Marais, J.S.C.**1944. Monofluoro-acetic acid, the toxic principle of “gifblaar”, *Dichapetalum cymosum*. Onderstepoort J of Vet Res. **20** 67–73.

24. **Murphy, C. D.** 2007. The application of 19F nuclear magnetic resonance to investigate microbial biotransformations of organofluorine compounds. OMICS: **11:**314-324.
25. **Nakamura, K., T. Noike, and J. Matsumoto.** 1986. Effect of operation conditions on biological Fe2+ oxidation with rotating biological contactors. Water Res. **20:**73-77.
26. **Ohandja, D. G., and D. C. Stuckey.** 2006. Development of a membrane-aerated biofilm reactor to completely mineralise perchloroethylene in wastewaters. J Chem Technol Biotech. **81:**1736-1744.
27. **Pedersen, K.** 1990. Biofilm development on stainless steel and PVC surfaces in drinking water. Water Res **24:**239-243.
28. **Peys, K., L. Diels, R. Leysen, and C. Vandecasteele.** 1997. Development of a membrane biofilm reactor for the degradation of chlorinated aromatics. Water Sci and Technol. **36:**205-214.
29. **Simoes, M., M. O. Pereira, S. Sillankorva, J. Azeredo, and M. J. Vieira.** 2007. The effect of hydrodynamic conditions on the phenotype of *Pseudomonas fluorescens* biofilms. Biofouling. **23:**249-258.
30. **Song, B., and L. G. Leff.** 2006. Influence of magnesium ions on biofilm formation by *Pseudomonas fluorescens*. Micro Res. **161:**355-361.
31. **Sousa, C., M. Henriques, J. Azeredo, P. Teixeira, and R. Oliveira.** 2008. *Staphylococcus epidermidis* glucose uptake in biofilm versus planktonic cells. World J Microbiol Biotechnol. **24:**423-426.
32. **Stewart, P. S.** 2003. Diffusion in biofilms. J Bacteriol. **185:**1485-1491.
33. **Twigg, L. E., and L. V. Socha.** 2001. Defluorination of sodium monofluoroacetate by soil microorganisms from central Australia. Soil Biol Biochem. **33:**227-234.
34. **van Loosdrecht, M. C., J. Lyklema, W. Norde, and A. J. Zehnder.** 1990. Influence of interfaces on microbial activity. Microbiol Mol Biol Rev. **54:** 75-87.
35. **Walker, J. R. L., and L. Bong Chui.** 1981. Metabolism of fluoroacetate by a soil *Pseudomonas SP*. and *Fusarium solani*. Soil Biol Biochem. **13:**231-235.
36. **Wobus, A., S. Ulrich, and I. Röske.** 1995. Degradation of chlorophenols by biofilms on semi-permeable membranes in two types of fixed bed reactors. Water Sci Technol. **32:**205-212.
37. **Wong, D. H., W. E. Kirkpatrick, D. R. King, and J. E. Kinnear.** 1992. Defluorination of sodium monofluoroacetate (1080) by microorganisms isolated from western Australian soils. Soil Biol Biochem. **24:**833-838.
38. **Wong, D. H., W. E. Kirkpatrick, D. R. King, and J. E. Kinnear.** 1992. Environmental-factors and microbial inoculum size, and their effect on biodefluorination of sodium monofluoroacetate (1080). Soil Biol Biochem **24:**839-843

Figure Captions

Figure 1: Schematic of Tubular Biofilm Reactor (TBR). Each section consists of a 40 cm of silicone tubing with a total reactor length of 160 m.

623 **Figure 2:** The utilization of fluoroacetate involves the enzymatic cleavage of the carbon-
624 fluorine bond with the production of glycolate. The specific utilization rate of glycolate q_g is
625 a combination of q_{an} where carbon is incorporated into cell (anabolism), q_{en} where carbon is
626 used to provide energy for growth, q_m where carbon is used to provide energy for the
627 maintenance of cellular function not associated with growth (maintenance of intracellular
628 osmotic potential) but excludes any glycolate that is produced but not utilized (O_m) and
629 represents the total carbon utilized. The specific fluoroacetate utilization rate includes q_{an}, q_e,
630 q_m and O_m and represents the total fluoroacetate degraded.
631
632 **Figure 3:** Fluoroacetate defluorination via haloacetate dehalogenase
633
634 **Figure 4:** Typical histogram of fluorescent intensity for planktonic cells, Multicycle software
635 was used to determine the B, C and D phases of the cell cycle. B phase cells have a single
636 copy of DNA, C phase cells are synthesising DNA and D phase cells have a double copy of
637 DNA and are predivision.
638
639 **Figure 5:** Specific fluoroacetate (●) and glycolate (○) utilization rates for planktonic and
640 specific fluoroacetate (■) and glycolate (□) utilization rates for biofilm cells at varying
641 specific fluoroacetate loading rates. Regression analysis shows the superior performance of
642 planktonic cells (slope=0.87, R^2=0.90) in comparison to biofilm cells (slope=0.57, R^2=0.91)
643 at specific fluoroacetate loading rates between 2 and 14 × 10^{-12} mM/CFU h. 95 % confidence
644 intervals (---) are shown.
645
646 **Figure 6:** Fluorescent images of biofilm stained with the respiratory indicator CTC (red) and
647 the DNA binding dye DAPI (A) and the corresponding depth profiles of the location of

respiratory activity and biomass within the biofilm (B) show that respiratory activity decreases towards the biofilm/bulk liquid interface.

Figure 7: Cell cycle distributions for (A) planktonic and (B) biofilm cells at a number of specific glycolate utilization rates. (□) B phase, (■) C phase and (▩) D phase. Standard deviations were determined from a minimum of three independent biological samples. Planktonic specific glycolate utilization rates between 4-8 and 8-12 mM/CFU h correspond to growth rates of between 0.1-0.12 and 0.14-0.18 h^{-1} respectively.

672 **Table 1.** Biofilm thickness, dry weight, CFUs, and density data after approximately 300 h of
673 growth on varying carbon loading rates. Carbon loading rates are used here and not
674 fluoroacetate loading rates to take it to account that some sections of the reactors have both
675 fluoroacetate and glycolate in the inlet feed.

676

Carbon loading rate (mM/h)	Initial reactor fluoroacetate concentration (mM)	Reactor section	Thickness (μm)	Dry weight (g/ 40 cm section)	CFU/ 40 cm section	Density (g/l)
0.000	10	4	12	0.0000	1.12×10^{9}	0.00
0.000	10	3	22	0.0016	6.48×10^{9}	18.5
0.000	20	4	29	0.0120	6.20×10^{9}	108
0.007	20	4	32	0.0128	1.68×10^{9}	80.0
0.017	10	2	150	0.0952	4.40×10^{10}	169
0.036	20	3	92	0.0624	1.91×10^{10}	181
0.036	20	3	85	0.0496	1.52×10^{10}	154
0.080	20	2	95	0.0728	8.81×10^{9}	202
0.081	20	2	136	0.0656	2.72×10^{10}	128
0.107	10	1	281	0.0696	4.56×10^{10}	65.0
0.168	20	1	120	0.0720	1.92×10^{10}	159
0.187	20	1	120	0.0872	1.36×10^{10}	192
0.304	50	4	134	0.0552	6.16×10^{9}	108
0.362	50	3	147	0.0768	4.40×10^{9}	138
0.412	50	2	96	0.0728	1.12×10^{10}	201
0.509	50	1	110	0.0648	1.92×10^{10}	156

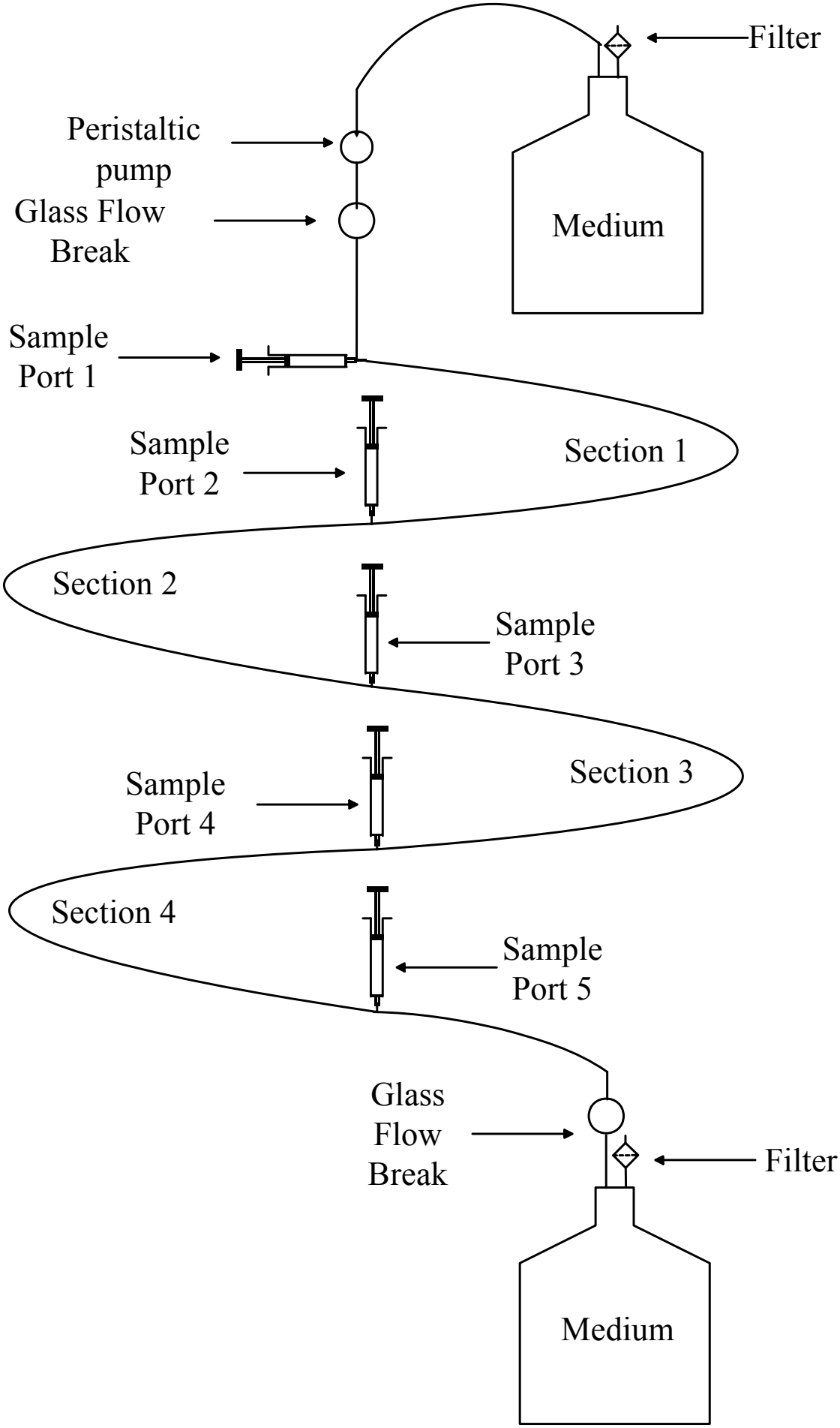
Filter
Peristaltic pump
Glass Flow Break
Medium
Sample Port 1
Sample Port 2
Section 1
Section 2
Sample Port 3
Sample Port 4
Section 3
Section 4
Sample Port 5
Glass Flow Break
Filter
Medium

Figure: 1

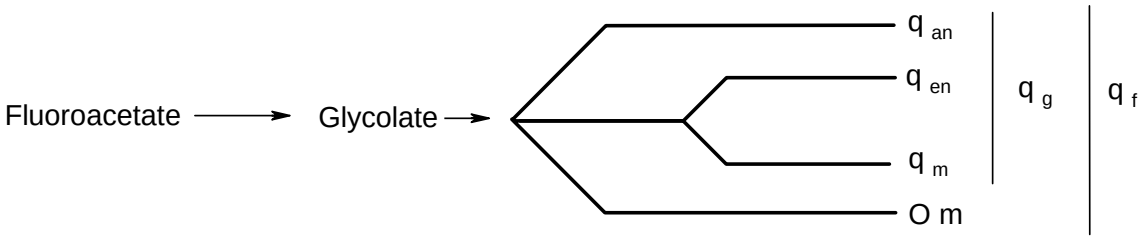

Figure: 2

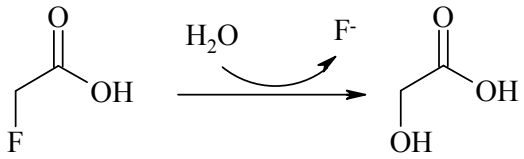

Figure: 3

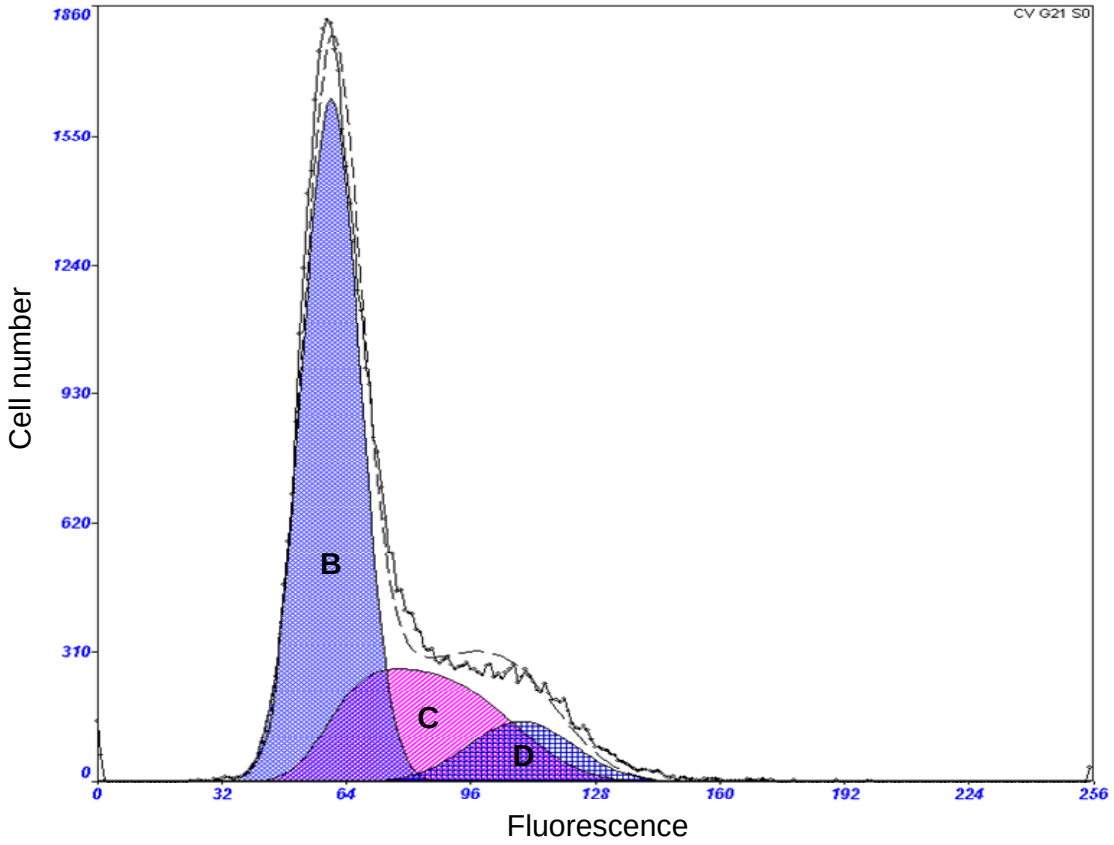
CV G21 S0
1860
1550
1240
930
620
310
0
Cell number
B
C
D
0
32
64
96
128
160
192
224
256
Fluorescence

Figure: 4

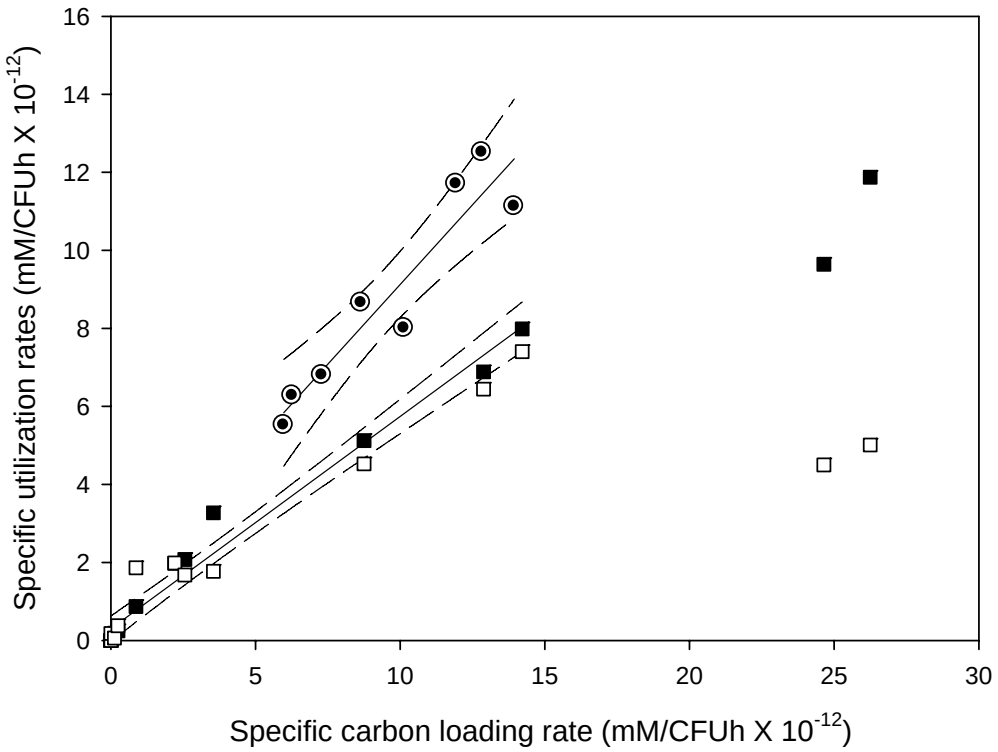
Specific utilization rates (mM/CFUh X 10-12)
Specific carbon loading rate (mM/CFUh X 10-12)
0
2
4
6
8
10
12
14
16
0
5
10
15
20
25
30

Figure: 5

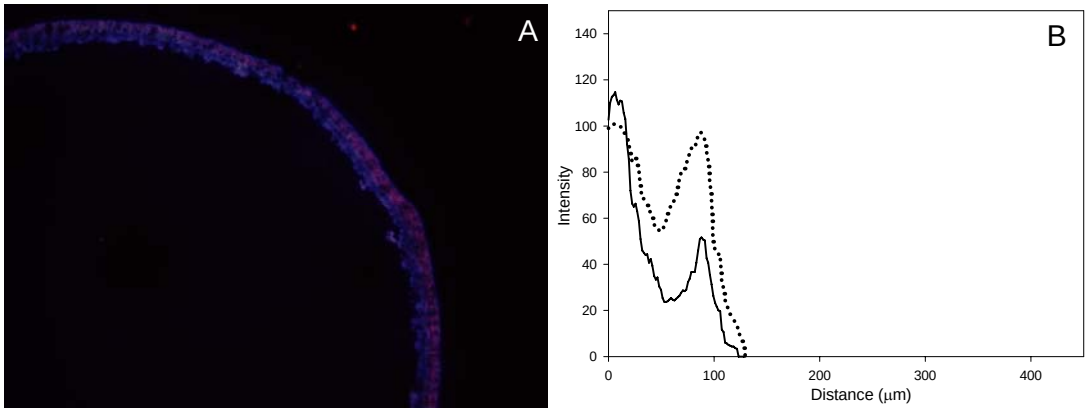
A
B
Intensity
Distance (μm)
0
20
40
60
80
100
120
140
0
100
200
300
400

Figure: 6

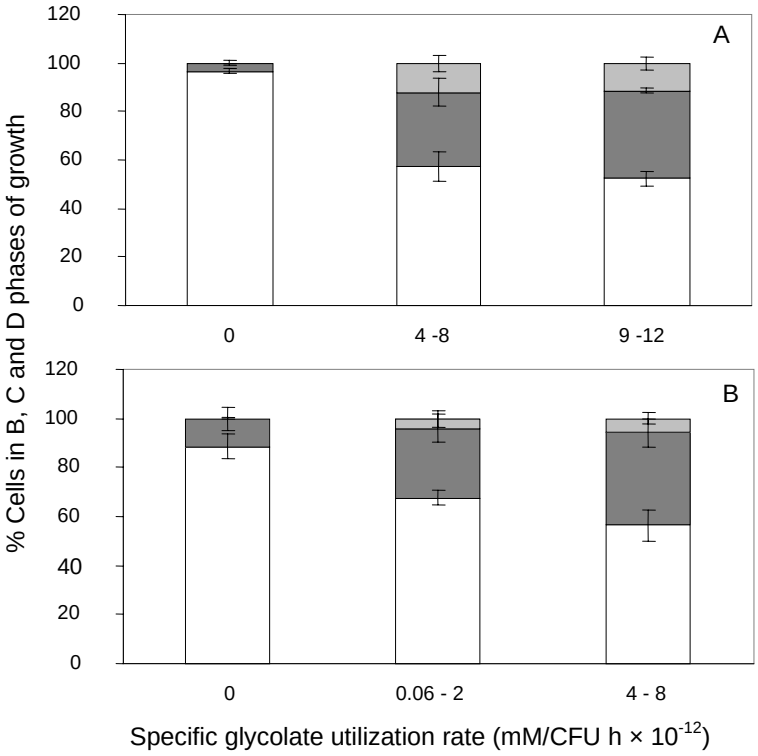

Figure: 7